Green Chemistry

Accepted Manuscript

ROYAL SOCIETY OF CHEMISTRY

www.rsc.org/greenchem

Journal Name

RSCPublishing

COMMUNICATION

Use of ultrasonic cavitation for near-surface structuring of robust and low-cost AlNi catalysts for hydrogen production

Cite this: DOI: 10.1039/x0xx00000x

Received 00th January 2012,
Accepted 00th January 2012

DOI: 10.1039/x0xx00000x

www.rsc.org/

P. V. Cherepanov[a], I. Melnyk[a], E. V. Skorb[b], P. Fratzl[b], E. Zolotoyabko[c], N. Dubrovinskaia[d], L. Dubrovinsky[e], Y. S. Avadhut[f], J. Senker[f], L. Leppert[g], S. Kümmel[g], and D. V. Andreeva[a]*

Ultrasonically induced shock waves stimulate intensive interparticle collisions in suspensions and create large local temperature gradients in AlNi particles. These trigger the phase transformations at the surface rather than in the particle interior. We show that ultrasonic processing is an effective approach for developing the desired compositional gradients in nm-thick interfacial regions of metal alloys and formation of effective catalysts toward hydrogen evolution reaction.

The hydrogen evolution reaction (HER) is an important technological process for the production of molecular hydrogen through water splitting.[1] Catalysts for the HER reversibly bind hydrogen to their surface.[2] Rapid HER kinetics was observed when utilizing expensive metal catalysts.[3-5] Recently, it was shown that near-surface and surface alloys potentially can have excellent catalytic properties for hydrogen production.[6,7] However, up to now such alloys were prepared by time and energy consuming deposition-annealing procedure using transition metals and Pt(111) surface.[7,8] In this paper, we propose novel and efficient ultrasound-assisted approach to the manipulation of metal alloy surface at atomic level. We use shock impact of billions of collapsing cavitation bubbles during ultrasonic processing for near-surface phase transformation in AlNi particles; the transformation which can hardly be achieved by conventional methods.

According to Norskov et al.,[2] the free energy of hydrogen adsorption (ΔG_{H^*}) on a catalyst surface is a reliable descriptor of catalytic activity for a variety of compounds. The value of ΔG_{H^*} close to zero indicates that hydrogen intermediates are bound neither too strongly nor too weakly to the catalyst surface. In order to disclose which intermetallic phase in AlNi alloys could potentially be active in HER, we calculated the free energy of hydrogen adsorption for AlNi intermetallics (see the Supporting Information for details of our Density Functional Theory (DFT) calculations).

Fig. 1 demonstrates that the HER can proceed nearly thermo-neutrally at the (100)-planes of Al_3Ni_2. In contrast, the value of ΔG_{H^*} for the Al_3Ni(010) surface plane is more negative due to pronounced surface reconstruction upon hydrogen adsorption and, hence, this plane can be considered equally inactive as pure Ni.

The obtained results, therefore, indicate that the Al_3Ni_2(100) phase in our intermetallic system is expected to be the most active for electrocatalysis. By measuring the particles' activity in HER, we can evaluate how accessible the surface of the Al_3Ni_2(100) phase is for H-adsorption.

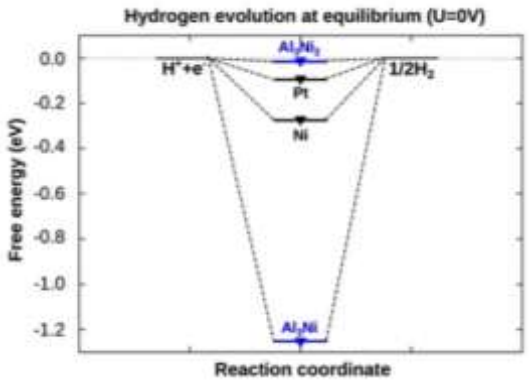

Fig. 1 Calculated free energy diagram for hydrogen evolution at a potential U=0 relative to the standard hydrogen electrode at pH=0. Values for Pt and Ni were taken from Ref.[33]. Al_3Ni_2(100) shows a high potential for the hydrogen evolution reaction.

In order to experimentally evaluate the predicted activity of the intermetallics during water splitting, we tested the functioning of bulk commercial Al_3Ni_2 and Al_3Ni compounds in HER. The HER current/potential profiles are shown in **Fig. 2a**.

It is well known that hydrogen production at the surface of the efficient electrocatalyst must be characterized with closer to zero overpotential and high current density output. As predicted by our DFT calculations, our experimental results clearly show that the beneficial phase for water splitting is Al_3Ni_2, whereas the Al_3Ni phase binds H too strongly. However, the measured electrocatalytic characteristics of the unstructured bulk Al_3Ni_2 are not as spectacular as predicted by DFT calculations, probably due to the low accessibility of the active Al_3Ni_2(100) planes for hydrogen adsorption. Therefore, the decisive question is whether it is possible to find an efficient method for structuring of the Al_3Ni_2 phase.

Recently, it has been argued that structuring of near-surface regions in metal alloys is of great importance for achieving enhanced catalytic activities of intermetallic compounds.[6] High electrocatalytic activity was observed[7,8] for structured compounds with enhanced accessibility of potentially active crystal planes. Thus, the relatively poor (higher onset overpotential and lower apparent current density values) electrocatalytic behavior of Al_3Ni_2 can be enhanced by structuring of the AlNi alloys containing the Al_3Ni_2 hexagonal phase. Upon controlled structuring of intermetallic phases in the AlNi alloy, we do achieve preferential orientation of the (100) hexagonal crystal planes at the surface and, thus, the enhancement of the Al_3Ni_2 activity toward HER.

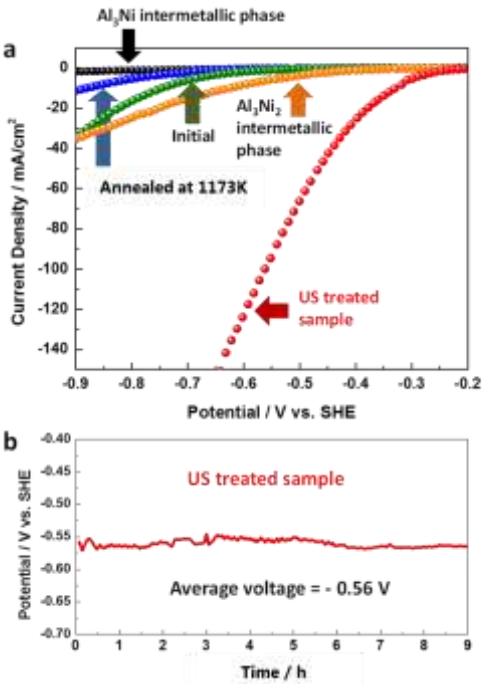

Fig. 2 HER current – potential profiles for the initial and ultrasonically modified AlNi (50 wt.% Ni) alloys, bulk commercial Al_3Ni and Al_3Ni_2 phases, as well as AlNi alloy annealed at 1173K (a). Galvanostatic HER profile for ultrasonically modified AlNi (50 wt.% Ni) alloy (b).

According to the AlNi binary phase diagram[9,10] (**Fig. S1, ESI**) and the previous works on electrocatalytic application of AlNi compounds[11-14] the best AlNi candidates for the catalyst preparation are AlNi alloys with nearly 50 wt.% of Ni. The Rietveld refinement of the powder X-ray diffraction (PXRD) patterns of the investigated samples showed that this alloy is a mixture of Al (2 wt.%), Al_3Ni (43 wt.%), and Al_3Ni_2 (55 wt.%). However, during alloy preparation from melt, the desirable clustering of Al_3Ni_2 at the surface of Al_3Ni is kinetically restricted due to the preferable nucleation of the Al_3Ni phase on the surface of already formed Al_3Ni_2 phase. At the same time, the formation enthalpies are $\Delta H \approx -65$ kJ/mol and $\Delta H \approx -45$ kJ/mol for Al_3Ni_2 and Al_3Ni, respectively.[15] This means that the Al_3Ni_2 phase is thermodynamically more stable than the Al_3Ni phase. Indeed, according to the equilibrium phase diagram at 1124 K, the Al_3Ni phase can be transformed into the Al_3Ni_2 phase ($\mathbf{Al_3Ni \xrightarrow{1124K} Al_3Ni_2 + L_{15{,}3\ at.\ \%\ Ni}}$).[10] Thus, in principle, it should be possible to trigger the desirable phase transformation by conventional heating. However, the obtained product is not electrochemically active (**Fig. 2a**, blue curve), since the highly active surface planes of the (100)-type remain undeveloped. Therefore, a novel technological solution is required for dedicated near-surface phase transformations in AlNi particles.[16-18]

Technologically fast and controllable local heating of a surface can be achieved by the impact of micron-size high-energy cavitation bubbles.[19] Collapsing of cavitation bubbles that are generated in ethanol by high power ultrasound (HPUS) at 20 kHz induces shock waves and intensive turbulent flow.[20,21] In suspensions cavitation triggers intensive interparticle collisions that results in extremely rapid local rise of the surface temperature of the sonicated particles followed by the quenching down to the surrounding medium temperature of 333 K. In this paper, we investigate the HPUS-induced structuring of the intermetallic phases by using ~140 µm particles of AlNi alloys suspended in ethanol (for details see **ESI**). The catalyst preparation route via ultrasonication is sketched in **Fig. 3** and explained in the **ESI, Fig. S3.**

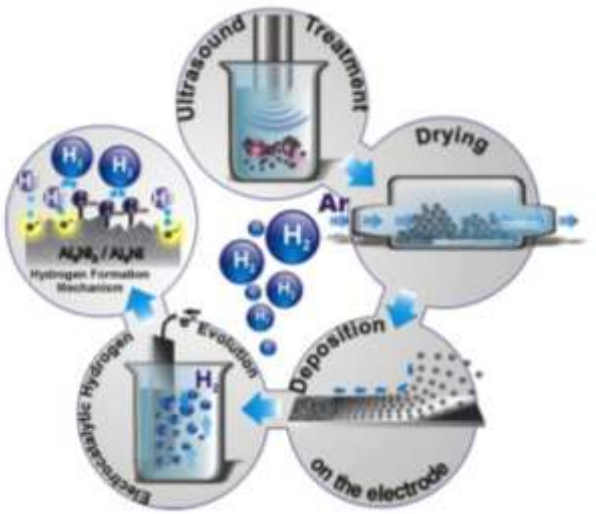

Fig. 3 Schematic illustration of the catalyst preparation procedure. First 10 wt.% suspensions of alloy particles (~140 µm) are sonicated in ethanol at a frequency of 20 kHz and an intensity of 140 Wcm^{-2} for 1 h. This processing results in the activation of the catalyst surface (change in crystal structure, phase composition, and morphology). After that the modified particles are centrifuged and dried in Ar atmosphere. The dried particles are deposited on a substrate and their electrocatalytic activity is evaluated.

Indeed, the HPUS treatment of AlNi particles causes remarkable modification of morphology and surface composition in the AlNi alloys. The compositional and morphological changes are clearly visible, when comparing the energy-dispersive X-ray spectroscopy (EDS) results, the ^{27}Al solid state nuclear magnetic resonance (NMR) spectra, X-ray photoelectron spectroscopy (XPS) data and the scanning electron microscopy (SEM) images. The SEM pictures (**Fig. 4b**) show the surface roughening after the HPUS treatment. This surface modification is clearly revealed in comparison with the relatively smooth particle surface before the treatment (**Fig. 4a**). Furthermore, EDS analysis of the surface composition of the particles before and after sonication shows a mixture of phases near the surface of pristine particles (**Table S2, ESI**). On the contrary, after the HPUS treatment (**Fig. 4c, d**), EDS detects the presence at the surface a solitary Al_3Ni_2-phase. Additional evidences of the microstructure refinement in the alloys after the HPUS treatment are provided by selected area electron diffractions (SAED) (see inserts in **Fig. 4a, b**). The ultrasonically induced clustering of intermetallic phases in the modified AlNi particles is also schematically illustrated in **Fig. 4a, b**.

The EDS results, as well as the ^{27}Al solid state NMR spectra (**Fig. 4e,f**) and XPS surface analysis (**Fig. 4 g,h**), provide clear evidence of the spatial re-distribution of the phases within metallic particles after the treatment.

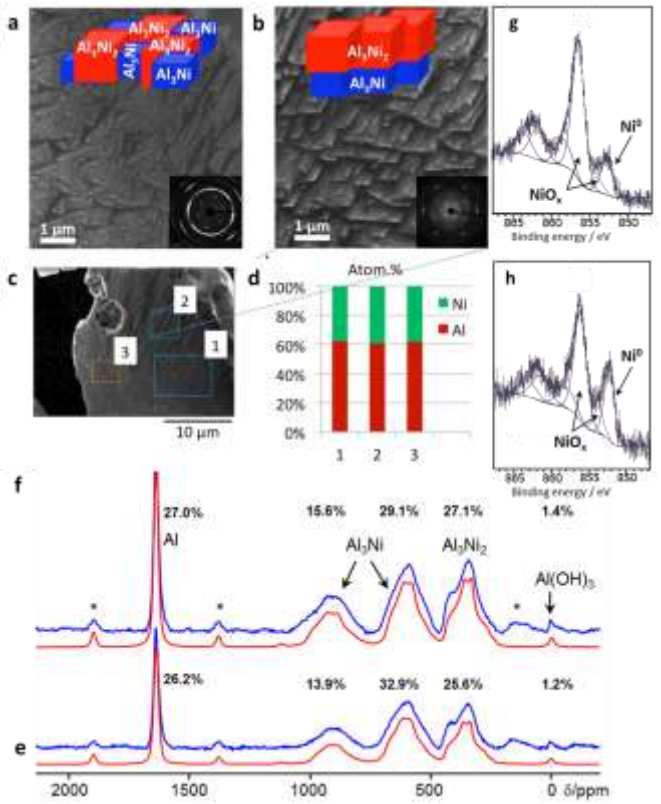

Fig. 4 Scanning electron microscopy images taken from the surface of AlNi (50 wt.% Ni) before (a) and after (b) ultrasonication. The inserts show selected area electron diffractions, which demonstrates the tendency to form larger intermetallic crystals after the HPUS treatment. The sketches illustrate the random phase distribution in the initial AlNi particles and the preferential clustering of the Al_3Ni_2 phase upon the HPUS treatment. Energy dispersive X-ray analysis of the metal surface after ultrasonication proves the formation of Al_3Ni_2 at the surface, where aluminum to nickel is 3:2 (c,d). ^{27}Al MAS NMR spectra (blue) of sonicated in ethanol (f) as well as pristine AlNi (e) and their corresponding simulated spectra (red) are shown below, respectively. Additionally, the relative intensities of each resonance are indicated (see also **Tab. S1**, **ESI**). The asterisks denote spinning sidebands. X-ray photoelectron spectra of the initial (g) and modified samples (h).

The EDS results, as well as the ^{27}Al solid state NMR spectra and XPS surface analysis, provide clear evidence of the spatial re-distribution of the phases within metallic particles after the treatment. Due to the skin effect (**see ESI**) the penetration depth of rf fields into conducting and magnetic materials is limited. Thus the ^{27}Al NMR spectra (**Fig 4e,f**) enhance the surface content of the AlNi alloy before and after ultrasonication. Both materials exhibit five different resonances (**Fig 4e,f**) which are assigned on the basis of the observed chemical shift. The main contribution arise from metallic Al (5.7 / 5.9 wt.%), Al_3Ni (52.6 / 50.1 wt.%), Al_3Ni_2 (40.9 / 43.1 wt.%), and $Al(OH)_3$ (0.8 / 0.9 wt.%) before and after sonication. While the Al as well as Al_3Ni ratios are slightly higher compared to the results of the PXRD analysis and on the other hand Al_3Ni_2 ratio is lower. This indicates a slight enrichment of Al and Al_3Ni at the surfaces of the alloy particles compared to the bulk composition. Interestingly, sonication increases the surface content of Al_3Ni_2 from 41 to 43 wt.%. In parallel the percentage of Al_3Ni decreases from 52.6 to 50.1 wt.% leading to a decreased Al_3Ni / Al_3Ni_2 ratio from 1.3 to 1.15. This finding supports the hypothesis that Al_3Ni transforms slowly in Al_3Ni_2 during sonication. In contrast, the PXRD patterns showed that the sonication negligibly affected the bulk ratio of the phases in the samples. Furthermore, XPS surface analysis showed the increased concentration of Ni^0 at the surface (**Fig. 4h**) upon sonication of AlNi alloy particles in ethanol that also might confirm the formation of the more Ni-enriched Al_3Ni_2 phase comparing to Al_3Ni that covers the unmodified surface (**Fig. 4g**).

The formation of the Al_3Ni_2 phase on the alloy surface is possible if cavitation bubbles can heat the surface to above 1124 K. At this temperature the catalytically inactive Al_3Ni phase is transferred into the beneficial Al_3Ni_2 phase. The spectroscopic surface analysis before and after the HPUS treatment reveals the formation of the Al_3Ni_2 phase and, thus, proves local surface heating up to ~ 1124 K.

The development of the ultrasonically induced temperature gradient within the particles can stimulate additional crystal growth. We analyzed the PXRD patterns (**Fig. S4, ESI**) and calculated the crystallite sizes before and after the HPUS treatment using the Williamson-Hall (W-H) method[23-25] (for details, see **ESI**). According to our estimations, the Al_3Ni_2 and Al_3Ni crystallites in the HPUS treated AlNi are nearly twice as large (131 nm for Al_3Ni_2; 113 nm for Al_3Ni), as compared to pristine particles (87 nm for Al_3Ni_2; 56 nm for Al_3Ni). Assuming diffusion-controlled crystal growth during the treatment period (1 h), we estimate the diffusion rate in the AlNi (50 wt.% of Ni) to be about $2x10^{-18}$ m^2/s. The reference experiments (heating the particles in an oven for 1 h at different temperatures (for details see **Fig. S5**, Supporting Information) showed that the observed atomic diffusion proceeds at an average temperature in the particle interior that is equal to about T ≈ 823K.

Surface structuring via ultrasonication increases the accessibility of the DFT-predicted beneficial Al_3Ni_2(100) phase for H adsorption, which in turn should enhance the catalytic efficiency toward HER. In fact, we did observe outstanding improvement of the electrocatalytic properties (**Fig. 2a**) of AlNi particles after ultrasonication. The onset overpotential vs. SHE is significantly lowered to -0.25 V as compared to -0.65 V for pristine AlNi alloy particles. At the same time, the apparent current density values are strongly enhanced. For example, a drastic (more than 200-fold) increase in the current density was observed at an onset overpotential value of -0.4 V and was found to be 28.19 mA/cm^2 (HPUS-treated) as compared to 0.13 mA/cm^2 (initial).

Another very important parameter for evaluating the material's electrocatalytic performance is the exchange current density (i0), which reflects the intrinsic rate of electron transfer between the electrocatalyst's surface and the analyte. Therefore, we replotted the HER current/potential profiles in the Tafel coordinates and calculated i0-values for both the pristine and the HPUS-treated AlNi alloy particles. The calculated i0-value of 17.37 mA/cm^2 for the HPUS-modified alloy particles is three orders of magnitude higher than for the untreated ones ($0.016mA/cm^2$). All in all, our study shows that HPUS is a unique technological approach for producing the low-cost and efficient AlNi catalyst for water splitting. The ultrasonically generated AlNi catalyst is very robust and exhibits excellent stability in electrochemical use (**Fig. 2b**).

Conclusions

Using density functional theory we first predicted that the Al_3Ni_2 phase is potentially effective in hydrogen evolution reaction. However, bulk unstructured Al_3Ni_2 compounds demonstrated relatively low efficiency due to a low accessibility of the favorable

(100) atomic plane. We propose structuring of AlNi alloys containing the Al_3Ni_2 phase as an efficient and low cost technological approach for enhancing the accessibility of the Al_3Ni_2(100) planes that are active in hydrogen adsorption. The formation of the Al_3Ni_2 phase on the surface of AlNi alloys is kinetically restricted, but we demonstrate that processing of the metal surface by ultrasonically generated cavitation bubbles creates large local temperature gradients in the metal particles. These stimulate the desired phase transformations at the surface rather than in the particle interior. In particular, we show that collapsing cavitation bubbles heat the surface above 1124K, thus, triggering the near-surface transformation of the catalytically inactive Al_3Ni phase into beneficial Al_3Ni_2. In the particle interior, the estimated mean temperature reaches 824K, which is well below the phase transition temperature, but still enough for substantial solid-state diffusion and crystal growth. This simple, fast, and effective ultrasonic approach toward directed surface modification can be extended to other intermetallic systems for sustainable energy generation.

Experimental

The AlNi (50 wt.% Ni) alloy was prepared by melting Al (99.99% purity grade) and nickel (99.99% purity grade) foils (purchased from Sigma-Aldrich) using a Mini ARC melting device MAM-1 (Edmund Bühler Gmbh), TIG 180 DC. The HPUS treatment of AlNi alloy particles was performed by a Hielscher UIP1000hd, (Hielscher Ultrasonics GmbH, Germany) at operating frequency of 20 kHz. Electrochemical characterization was accomplished in a three electrode cell using 510 V10 Potentiostat/Galvanostat in 1M H_2SO_4 electrolyte. PXRD accompanied by Rietvild refinement, SEM and energy-dispersive EDS and solid state ^{27}Al NMR[26] were employed to verify the phase composition of the prepared AlNi alloys. TEM was used to obtain SAED patterns. DFT calculations were performed using the Vienna ab-initio Simulation Package.[27-32] Detailed information regarding sample preparation, ultrasound treatment, characterization methods, and calculations, is available in the ESI.

Acknowledgement

This work was financially supported by the A11, B1 and C1 projects of SFB 840. The authors thank to Dr. Beate Förster and Martina Heider (University of Bayreuth) for the SEM and EDS measurements, Carmen Kunnert for the TEM and ED measurements, Sebastian Koch, Bernd Putz, and Dr. Wolfgang Millius (Inorganic Chemistry I, University of Bayreuth) for assistance with XRD measurements, Katharina Schiller, Matthias Daab and Anna Kollath for help with samples' preparation.

Notes and references

[a] Physical Chemistry II, University of Bayreuth, DE-95440 Bayreuth, Germany, daria.andreeva@uni-bayreuth.de.

[b] Max Planck Institute of Colloids and Interfaces, DE-14424 Potsdam, Germany.

[c] Department of Materials Science and Engineering, Technion – Israel Institute of Technology, 32000 Haifa, Esrael.

[d] Materials Physics and Technology at Extreme Conditions, Laboratory of Crystallography, University of Bayreuth, DE-95440 Bayreuth, Germany.

[e] Bayrisches Geoinstitut, University of Bayreuth, DE-95440 Bayreuth, Germany.

[f] Inorganic Chemistry III, University of Bayreuth, DE-95440 Bayreuth, Germany.

[g] Theoretical Physics IV, University of Bayreuth, DE-95440 Bayreuth, Germany, e-mail: stephan.kuemmel@uni-bayreuth.de

† Electronic Supplementary Information (ESI) available: samples' preparation, PXRD, NMR data, EDS analysis and temperature experiments. See DOI: 10.1039/c000000x/

1 A. Züttel, A. Borgschulte, L. Schlapbach, Hydrogen as a future energy carrier, Wiley-VCH, Weinheim, Germany 2008.
2 E. Skulason, V. Tripkovic, M. E. Björketun, S. Gudmundsdottir, G. Karlberg, J. Rossmeisl, T. Bligaard, H. Jonsson, J. K. Nørskov, *J. Phys. Chem. C* 2010, **114**, 18182.
3 B. Hinnemann, P. G. Moses, J. Bonde, K. P. Jorgensen, J. H. Nielsen, S. Horch, I. Chorkendorff, J. K. Nørskov, *J. Am. Chem. Soc*. 2005, **127**, 5308.
4 T. F. Jaramillo, K. P. Jørgensen, J. Bonde, J. H. Nielsen, S. Horch, I. Chorkendorff, *Science* 2007, **317**, 100.
5 M. S. Faber, S. Jin, *Energy Environ. Sci*. 2014, **7**, 3519.
6 J. Greeley, M. Mavrikakis, *Nature Mater*. 2004, **3**, 810.
7 A. S. Bandarenka, A. S. Valera, M. Karamad, F. Calle-Vallejo, L. Bech, F. J. Perez-Alonso, J. Rossmeisl, I. E. L. Stephens, I. Cherkendorff, *Angew. Chem. Int. Ed.* 2012, **51**, 11845.
8 J. Knudsen, A. U. Nilekar, R. T. Vang, J. Schnadt, E. D. L. Kunkes, J. A. Dumesic, M. Mavrikakis, F. Nesenbacher, *J. Am. Chem. Soc.* 2007, **129**, 6485.
9 B. Predel, in Landolt-Borstein Group IV physical Chemistry, 12a, Springer, Berlin, Heidelberg 2006.
10 D. Batalu, G. Cosmeliata, A. Aloman, *Metalurgia Inter*. 2006, **11**, 36.
11 M. S. Wainwright, in Preparation of Solid Catalysts (Eds: G. Ertl, H. Knözinger, J. Weitkamp, Wiley-VCH, Weinheim, Germany, 1997.
12 D. Miousse, A. Lasia, *J. Appl. Elecrochem*. 1995, **25**, 592.
13 P. Los, A. Rami, A. Lasia, A. *J. Appl. Electrochem*. 1993, **23**, 135.
14 A. Rami, A. Lasia, *J. Appl. Electrochem*. 1992, **22**, 376.
15 D. Shi, B. Wen, R. Melnik, S. Yao, T. Li, *J. Solid State Chem*. 2009, **182**, 2664.
16 A. Ilbagi, P. D. Khatibi, H. Henein, R. Lengsdorf, D. M. Herlach, *J. Physics: Conference Series* 2011, **327**, 1.
17 D. M. Herlach, Phase transformation in multicomponent melts, John Wiley & Sons Ltd, 2009.
18 J. Dulle, S. Nemeth, E. V. Skorb, T. Irrgang, J. Senker, R. Kempe, A. Fery, D. V. Andreeva, *Adv. Func. Mater*. 2012, **22**, 3128.
19 B. J. H. Bang, K. S. Suslick, *Adv. Mater*. 2010, **22**, 1039.
20 K. S. Suslick, *Science* 1990, **247**, 1939.
21 S. J. Doktycz, K. S. Suslick, *Science* 1990, **247**,1067.
22 W. B. McNamara, Y. T. Didenko, K. S. Suslick, *Nature* 1999, **401**, 772.
23 T. Ungar, A. Revesz, A. Borbely, *J. Appl. Crystallogr*. 1998, **31**, 554.
24 K. Venkateswarlu, A. C. Bose, N. Rameshbabu, *Physica* 2010, **B405**, 4256.
25 A. K. Zak, W. H. A. Majid, M. E. Abrishami, R. Yousefi, *Solid State Sci.* 2011, **13**, 251.

26 R. Bhattacharyya, B. Key, H. Chen, A. S. Best, A. F. Hollenkamp, C. P. Grey, *Nature Mater*. 2010, **9**, 504.
27 G. Kresse, J. Furthmüller, *Comput. Mater. Sci.* 1990, **6**, 15.
28 G. Kresse, J. Furthmüller, *Phys. Rev*. 1996, **B54**, 11169.
29 P. E. Blöchl, *Phys. Rev*. 1994, **B50**, 17953.
30 J. K. Nørskov, T. Bligaard, A. Logadottir, J. R. Kitchin, J. G. Chen, S. Pandelov, U. Stimming, *J. Electrochem. Soc*. 2005, **152**, J23.
31 H. J. Monkhorst, J. D. Pack, *Phys. Rev*. 1976, **B13**, 5188.
32 B. Hammer, L. B. Hansen, J. K. Nørskov, *Phys. Rev*. 1999, **B46**, 7413.
33 J. Greeley, T. F. Jaramillo, J. Bonde, I. B. Chorkendorff, J. K. Nørskov, *Nature Mater*. 2006, **5**, 909.